Journal of Computational Physics **181,** 753–759 (2002)
doi:10.1006/jcph.2002.7163

Use of Routh's Correction in the Cloud-in-Cell Discrete Vortex Method

J. Malarkey and A. G. Davies

School of Ocean Sciences, University of Wales Bangor, Menai Bridge, Anglesey, LL59 5AB, United Kingdom
E-mail: j.malarkey@bangor.ac.uk

Received November 27, 2001; revised May 23, 2002

1. INTRODUCTION

Incompressible fluid flows comprising evolving, two-dimensional, vorticity fields are commonly represented by collections of discrete point vortices. The vorticity in the flow is generated at the solid boundaries of the motion in the so-called "physical plane." If the geometry of these boundaries is not simple, it is usual to calculate the flow field, including the trajectories of individual vortices, not in the physical plane but in a simpler "mapping plane." According to the rules of conformal mapping, there is a one-to-one correspondence between the two planes. However, in the classical, inviscid approach Routh's correction (see, for example, [2]) is required in the calculation of the trajectory of a vortex to ensure that the velocities are consistent between the mapping and physical planes at the location of the vortex. This correction arises because of the nature of the self-potential at the vortex location.

The "cloud-in-cell" (CIC) discrete vortex method [1] allows the velocity field resulting from a large number of point vortices to be calculated more efficiently than is possible in the inviscid (gridless) approach, by the introduction of a grid. Moreover the CIC method has also been used in conjunction with conformal mapping (see, for example, [7]). However, it is not clear *a priori* whether Routh's correction is required in this case, since the CIC method does not suffer from the self-potential problem. The purpose of this note is to investigate whether Routh's correction is required in the CIC method by considering a simple example.

Initially a general explanation is given of both the origin of Routh's correction in the inviscid method and how advection of a single vortex is performed in the mapping plane in both methods. This is followed by a brief explanation of the CIC method and by a particular example of a row of vortices moving over a rippled boundary, with one vortex being present per ripple wavelength.

2. ROUTH'S CORRECTION IN THE INVISCID METHOD

Consider a mapping function $z = f(\zeta)$ that satisfies the Cauchy–Riemann conditions ($\partial x/\partial \xi = \partial y/\partial \chi$ and $\partial x/\partial \chi = -\partial y/\partial \xi$) where $z = x + jy$, $\zeta = \xi + j\chi$, $j = (-1)^{1/2}$,

0021-9991/02 $35.00

and x and ξ are the horizontal and y and χ the vertical coordinates in the physical and mapping planes, respectively. Then the horizontal and vertical velocities in the physical plane, u_z and v_z, are related to those in the mapping plane, u_ζ and v_ζ, by

$$u_z - jv_z = \zeta'(u_\zeta - jv_\zeta), \tag{1}$$

where $\zeta' = d\zeta/dz$, $u_z - jv_z = d\Omega/dz$, $u_\zeta - jv_\zeta = d\Omega/d\zeta$, and Ω is the complex potential. Equation (1) holds only if the flow is irrotational, which is not the case at the centre of a point vortex. It is Routh's correction that restores consistency between the velocities at the vortex positions in the two planes when Eq. (1) breaks down. Routh's correction is explained below.

At a particular instant, let there be a vortex of circulation Γ_0 located at $z = z_0$, and correspondingly at $\zeta = \zeta_0$, in the physical and mapping planes, respectively. The complex potential in the two planes, on the basis of which vortex advection occurs, is the same such that

$$\Omega = \Omega_z - j\Gamma_0(2\pi)^{-1}\log(z - z_0) = \Omega_\zeta - j\Gamma_0(2\pi)^{-1}\log(\zeta - \zeta_0), \tag{2}$$

where $\Gamma_0 > 0$ for anticlockwise circulation and Ω_z and Ω_ζ are the complex potentials in the z and ζ planes excluding the vortices at $z = z_0$ and $\zeta = \zeta_0$, respectively. Clements [2] used a Taylor expansion to show that the vortex velocity in the physical plane, $d\Omega_z/dz = u_{z0} - jv_{z0}$ from Eq. (2), could be expressed as

$$u_{z0} - jv_{z0} = \zeta_0'\left[\frac{d\Omega_\zeta}{d\zeta} - j\frac{\Gamma_0\zeta_0''}{4\pi\zeta_0'^2}\right]. \tag{3}$$

This is an exact result relating the physical plane velocity to mapping plane quantities, in which the second term in the square brackets is Routh's correction. Thus the square-bracketed term is the conjugate of $u_{\zeta 0} + jv_{\zeta 0}$, the mapping plane velocity at ζ_0, by comparison with Eq. (1).

3. ADVECTION IN THE MAPPING PLANE

In calculations of vortex migration, when a vortex position in one plane is advanced during a defined time interval using the velocity at its location, the corresponding vortex in the other plane must move accordingly. In practice, the vortex velocity in the mapping plane, $u_{\zeta 0} + jv_{\zeta 0}$, is not the velocity, given by $d\zeta_0/dt$ where t is time, used to advect the vortex in the mapping plane because advection performed in the mapping plane must be consistent with "true" advection occuring in the physical plane. Since $u_{z0} + jv_{z0} = dz_0/dt$, and also from the chain rule $d\zeta_0/dt = \zeta_0' dz_0/dt$, where $u_{z0} - jv_{z0} = \zeta_0'(u_{\zeta 0} - jv_{\zeta 0})$ from Section 2, then $d\zeta_0/dt = |\zeta_0'|^2(u_{\zeta 0} + jv_{\zeta 0})$. Thus, in finite difference form, the change in position of the vortex, $\Delta\zeta_0$, over a time interval, Δt, is given by

$$\Delta\zeta_0 = |\zeta_0'|^2\mathbf{u}_{\zeta 0}\Delta t, \tag{4}$$

where $\mathbf{u}_{\zeta 0} = u_{\zeta 0} + jv_{\zeta 0}$. Equation (4) allows the vortex to be advected in the mapping plane in a strictly consistent manner with advection of the equivalent vortex in the physical plane. For example, Eq. (4) was used by Longuet-Higgins [3], with $\mathbf{u}_{\zeta 0}$ calculated using the inviscid method, and by Smith and Stansby [7], with $\mathbf{u}_{\zeta 0}$ calculated using the CIC method.

4. THE CIC METHOD

The CIC method [1] provides an alternative way of calculating $\mathbf{u}_{\zeta 0}$ for a point vortex. Here the introduction of a grid allows the strength of each vortex to be temporarily credited to its neighbouring grid nodes. The distribution of all point vortices in the flow is then represented by a distribution of vorticity values over the entire grid. This allows the velocity at the grid nodes to be calculated via a streamfunction solution of Poisson's equation [1]. The velocity at the vortex locations, which is interpolated back from the grid node velocities, is then used to advect the vortices. At each time step, this process is repeated. In most applications (see, for example, [4, 7]), this "advective step" is alternated with a diffusive one, by imposing a random walk jump on the position of each vortex. However, in the present example, the "diffusive step" is not included so that a direct comparison can be made with the inviscid method. In anticipation of the example that follows, the explanation of the method given below considers only one vortex, but it should be understood that the same reasoning applies to many vortices.

In the mapping plane the grid is regular and Cartesian with cells of length $\Delta\xi$, and height $\Delta\chi$, and the grid node positions are given by $\zeta_{i,k} = \xi_i + j\chi_k$. The point vortex credits vorticity to the four grid nodes of the cell that contains it, say the i,kth, $i+1,k$th, $i,k+1$th, and $i+1,k+1$th nodes. In particular, the vorticity at the i,kth node, $\omega_{i,k}$, is given by

$$\omega_{i,k} = \Gamma_0 A_{i,k} (\Delta\xi \Delta\chi J_{i,k})^{-1}, \tag{5}$$

where $A_{i,k}$ is the area weighting factor and $J_{i,k} = |\zeta'_{i,k}|^{-2}$. Equivalent expressions may be written for the $i+1,k$th, $i,k+1$th, and $i+1,k+1$th nodes. The respective area weighting factors are given by

$$\begin{aligned} A_{i,k} &= (\Delta\xi - \delta\xi)(\Delta\chi - \delta\chi)/\Delta\xi\Delta\chi, & A_{i+1,k} &= \delta\xi(\Delta\chi - \delta\chi)/\Delta\xi\Delta\chi, \\ A_{i,k+1} &= (\Delta\xi - \delta\xi)\delta\chi/\Delta\xi\Delta\chi, & A_{i+1,k+1} &= \delta\xi\delta\chi/\Delta\xi\Delta\chi, \end{aligned} \tag{6}$$

where $\delta\xi + j\delta\chi$ is the vortex position within the cell. The vorticity distributed to the nodes now becomes the source term in Poisson's equation, which, in finite-difference form, is

$$\frac{\psi_{i+1,k} - 2\psi_{i,k} + \psi_{i-1,k}}{\Delta\xi^2} + \frac{\psi_{i,k+1} - 2\psi_{i,k} + \psi_{i,k-1}}{\Delta\chi^2} = -J_{i,k}\omega_{i,k}, \tag{7}$$

where $\psi_{i,k}$ is the streamfunction at the i,kth grid node. Solving Eq. (7) allows the velocities in the mapping plane at the grid nodes to be expressed as

$$\mathbf{u}_{\zeta i,k} = \frac{\psi_{i,k+1} - \psi_{i,k-1}}{2\Delta\chi} + j\frac{\psi_{i-1,k} - \psi_{i+1,k}}{2\Delta\xi}. \tag{8}$$

The vortex velocity is next interpolated from the neighbouring grid node velocities, back to the vortex position, using the same area weighting factors:

$$\mathbf{u}_{\zeta 0} = A_{i,k}\mathbf{u}_{\zeta i,k} + A_{i+1,k}\mathbf{u}_{\zeta i+1,k} + A_{i,k+1}\mathbf{u}_{\zeta i,k+1} + A_{i+1,k+1}\mathbf{u}_{\zeta i+1,k+1}. \tag{9}$$

This value of $\mathbf{u}_{\zeta 0}$ is then used in Eq. (4) to advect the vortices.

Christiansen [1] referred to Eqs. (4)–(9) as "a consistent set of interpolations in the sense that a single point vortex will not move in its own velocity field." However, this is not the

case for the inviscid approach unless the self-potential is removed, resulting in Routh's correction in the mapping plane, as described in Section 2.

5. A VORTEX MOVING OVER A RIPPLE

Thus far the two methods have been described in a general way. In this section, the specific case is considered of a single vortex moving over each ripple, in a two-dimensional domain with periodic lateral boundary conditions imposed above the ripple troughs.

A mapping function that satisfies the Cauchy–Riemann conditions and can be used to represent the region above a rippled bed with wavelength 2π [8] is given by

$$z = \zeta + j \sum_{n=0}^{N_\alpha} \alpha_n e^{jn\zeta}, \tag{10}$$

where $\alpha_n = a_n + jb_n$, and the ripple surface is represented by $\chi = 0$. Malarkey [4] showed that a specific symmetric sharp-crested ripple profile given by

$$y = h(1 - |x|/\pi)^2, \quad |x| \le \pi, \tag{11}$$

where h is the ripple height, can be adequately represented, without singularities in the mapping function derivatives, using Eq. (10) truncated at $N_\alpha = 9$, with $b_n = 0$. The mapping and physical planes for the sharp-crested ripple profile are shown in Figs. 1a and 1b. The ripple has a steep crest and a long flat trough, characteristic of sand ripples. This ripple shape is used in the following example.

In the inviscid method, the complex potential for horizontally periodic flow, comprising one vortex (at $\zeta = \zeta_0$) per ripple wavelength, is given by an infinite row of vortices spaced 2π apart, $\Omega = -j\Gamma_0(2\pi)^{-1}\log[\sin 1/2(\zeta - \zeta_0)]$ [5]. The resulting velocity in the mapping plane can be written

$$u_\zeta - jv_\zeta = -j\Gamma_0(4\pi)^{-1}[\cot 1/2(\zeta - \zeta_0) - \cot 1/2(\zeta - \zeta_0^*)], \tag{12}$$

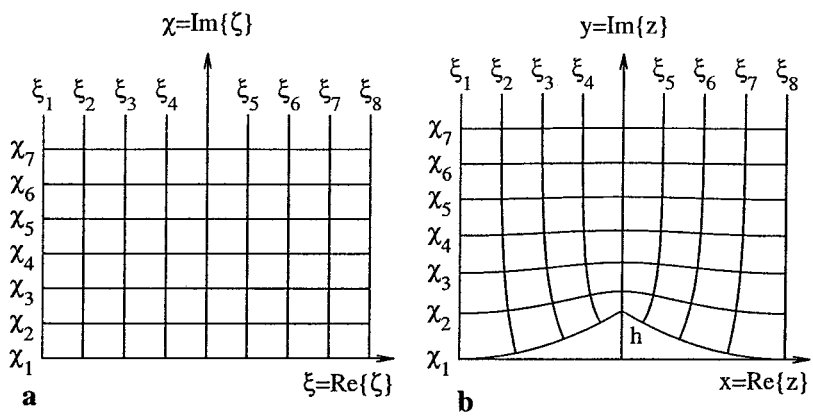

FIG. 1. Lines of constant ξ and χ in (a) the mapping plane and (b) the physical plane for a sharp-crested ripple.

where the second term in the square brackets is due to the image row located at ζ_0^* ($*$ represents a complex conjugate), which is required to ensure no flow though the bed. The image row will cause the vortex to be advected parallel to the bed and, from Eq. (3), $\mathbf{u}_{\zeta 0}$ is given by

$$\mathbf{u}_{\zeta 0} = \frac{\Gamma_0}{4\pi}\left[\coth 1/2\chi_0 - j\frac{\zeta_0''}{\zeta_0'^2}\right]^*. \tag{13}$$

In the CIC method, the size of the grid is $2\pi \times \pi$ with 32×64 intervals, $\xi_i = i\Delta\xi - \pi$, and $\chi_k = k\Delta\chi$ ($0 \le i \le 32$, $0 \le k \le 64$, $\Delta\xi = \pi/16$, and $\Delta\chi = \pi/64$). Equation (7) has been solved subject to the following boundary conditions: horizontally periodic flow, $\psi_{0,k} = \psi_{32,k} \Rightarrow \psi_{-1,k} = \psi_{31,k}$ and $\psi_{33,k} = \psi_{2,k}$; no flow through the bed, $\psi_{i,0} = 0$; and a specified free-stream velocity, together with zero velocity shear at the top of the grid, $\psi_{i,64} = \psi_{i,63} + 2\Delta\chi u_{\zeta i,64}$, where $u_{\zeta i,64} = u_\zeta(\xi_i + j\pi)$ from Eq. (12), and $\psi_{i,64} = 1/2(\psi_{i,63} + \psi_{i,65})$. The resulting matrix is solved using the conjugate gradient method [6]. Also it is necessary to assume that $\psi_{i,-1} = -\psi_{i,j}$ for the grid node velocity, Eq. (8), to represent a local minimum in u_ζ in Eq. (12) along the bed ($\chi = 0$) (this condition together with $\psi_{i,0} = 0$ has the equivalent effect of the image row of vortices in the inviscid method). With a suitably small time interval, such that the vortex takes several advective steps to cross the horizontal distance equivalent to a single grid cell in the mapping plane, each method for calculating $\mathbf{u}_{\zeta 0}$ can be used in Eq. (4) and the results can be compared directly.

6. RESULTS

In Figs. 2a–2f the position of the vortex in the physical plane and the velocity of the vortex at its position in the mapping plane are compared between the two methods as a single vortex moves over the ripple profile, from left to right starting above the trough at $\zeta_0 = -\pi + 3.5j\Delta\chi$ ($h = 0.32\pi$ and $\Gamma_0 = 1$). The CIC method results are represented by the solid lines and the inviscid method, which includes Routh's correction, by the dotted lines. The results from the inviscid method in each pair of plots (a and b, c and d, and e and f) are the same. It can be seen that agreement between the two approaches is very good as long as Routh's correction is included in the CIC method (Figs. 2b, 2d, and 2f). Without Routh's correction (Figs. 2a, 2c, and 2e), the vortex trajectory is too close to the ripple crest (Fig. 2a) because no vertical velocity is predicted in the mapping plane (Fig. 2e). This, in turn, results in much larger variations in the horizontal mapping plane velocity (Fig. 2c) compared with the variations that occur when Routh's correction is included.

Figures 2c and 2d show a small periodic "wobble" in u_ζ from the CIC method, with a characteristic wavelength of $\Delta\xi$, superimposed on the general variation in velocity associated with the vortex position above the ripple. This relates to the location of the vortex within the grid cell. The wobble is maximum when the vortex is located halfway between two vertical nodes, and minimum when it is at the centre of the grid cell. The effect is due to the differing spread of circulation between the four nearest nodes as a result of the interpolation scheme (see Section 4). Despite this wobble, the vortex advances over the ripple at approximately the same rate in the two methods when Routh's correction is included.

The requirement for Routh's correction in the CIC method may be explained as follows. Mathematically, Routh's correction comes from the need to subtract the self-potential of the vortex being advected from the complete potential in the two planes, in order to avoid the

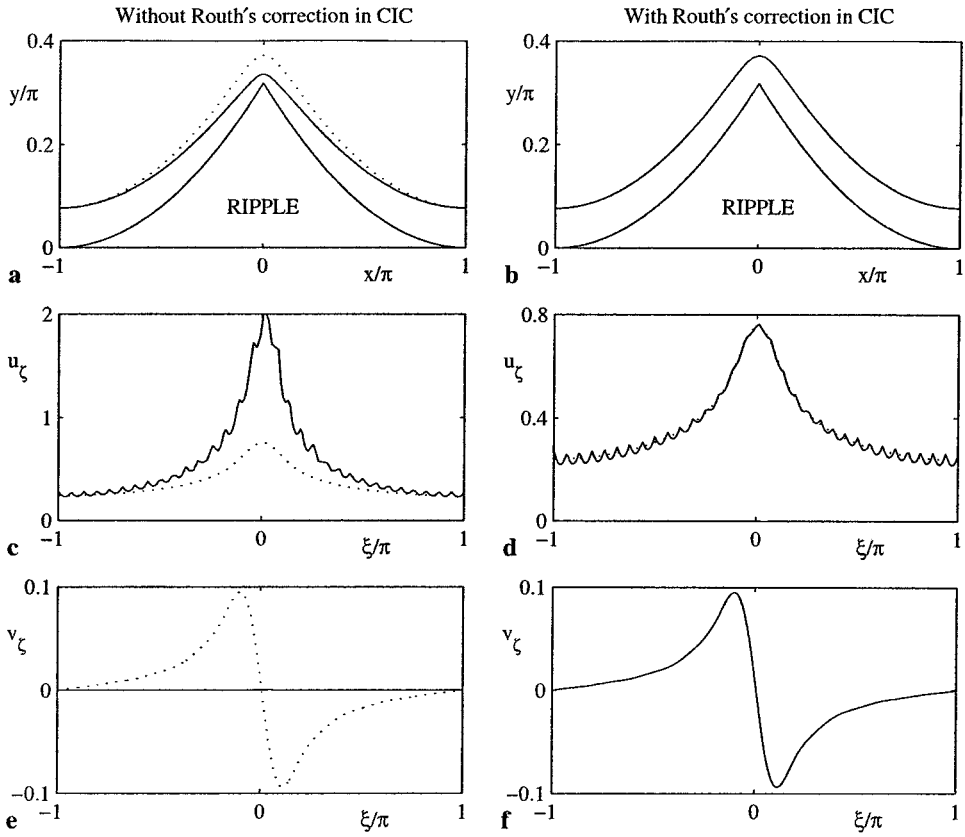

FIG. 2. Vortex trajectories in the physical plane (a, b) and horizontal (c, d) and vertical (e, f) velocities at the vortex location in the mapping plane for the CIC method (solid line) without and with Routh's correction, respectively, for a sharp-crested ripple. The results from the inviscid method (dotted lines), which includes Routh's correction.

problem of the velocity being infinite at the vortex centre (see Eq. (2)). Since this problem does not appear to arise in the CIC method, due to the distribution of vorticity to the grid nodes, it might be expected *a priori* that Routh's correction is not needed. However, at a more fundamental level, Routh's correction comes about because of rotational point vortices moving in an otherwise irrotational field, and the correspondence between the velocities in the mapping and physical plane relies on the assumption of irrotational flow. This is still the case for the CIC method when velocities are calculated in the mapping and physical planes. Since the CIC method is an approximation of the inviscid method, with the self-potential removed, it is in fact reasonable to conclude that the vortex velocities between the two planes are related in the same way as the vortex velocities based on potentials in the inviscid method.

7. CONCLUSIONS

The results have demonstrated that for the calculations of vortex trajectories made in the mapping plane, Routh's correction is required in the CIC method. Routh's correction

depends on the vortex circulation and on the first and second derivatives of the mapping function at the location of the vortex. It is difficult to quantify the importance of Routh's correction in results based on the CIC method where many vortices are involved, since this method is usually combined with a random walk component. On the one hand, unlike the specific case presented here, Routh's correction might be expected to have quite a small effect since the circulation of the vortex is usually small compared with the total circulation of the flow when there are may other vortices. On the other hand, there are regions of the mapping plane domain where the derivatives of the mapping function can be quite large, for instance near sharp corners. In these regions it is likely that Routh's correction is more important. The additional computational cost of including the correction term will usually be quite small.

ACKNOWLEDGMENTS

This work was partly funded by the U. K. Ministry of Agriculture Fisheries and Foods under Contract CSA 3156 and also by the European Union as part of the MAST III SEDMOC project, number MAS3-CT97-0115.

REFERENCES

1. J. P. Christiansen, Numerical simulation of hydrodynamics by the method of point vortices, *J. Comput. Phys.* **13**, 363 (1973).
2. R. R. Clements, An inviscid model of two-dimensional vortex shedding, *J. Fluid Mech.* **57**, 321 (1973).
3. M. S. Longuet-Higgins, Oscillating flow over steep and ripples, *J. Fluid Mech.* **107**, 1 (1981).
4. J. Malarkey, *Modelling Oscillatory Flow over Vortex Ripples Using the Discrete Vortex Method*, Ph.D. dissertation (University of Wales, Bangor, 2001).
5. L. M. Milne-Thompson, *Theoretical Hydrodynamics* (MacMillan, London, 1968).
6. W. H. Press, B. P. Flannery, S. A. Teulosky, and W. T. Vetterling, *Numerical Recipes, The Art of Scientific Computing*, FORTRAN version (Cambridge Univ. Press, Cambridge, U.K., 1989), p. 77.
7. P. A. Smith and P. K. Stansby, Viscous oscillatory flows around cylindrical bodies at low Keulegan-Carpenter numbers using the vortex method, *J. Fluids Struct.* **5**, 339 (1991).
8. H. Tanaka, A conformal mapping of a finite region bounded by wavy walls, *Proc. JSCE* **369**, 319 (1986).